Rapid Structural Analysis of a Synthetic Non-canonical Amino Acid by Microcrystal Electron Diffraction

Patrick R. Gleason [1,2], Brent L. Nannenga [3,4]* and Jeremy H. Mills [1,2]*

[1] School of Molecular Sciences, Arizona State University, Tempe, AZ, United States, [2] Center for Molecular Design and Biomimetics, The Biodesign Institute, Arizona State University, Tempe, AZ, United States, [3] Chemical Engineering, School for Engineering of Matter, Transport and Energy, Arizona State University, Tempe, AZ, United States, [4] Center for Applied Structural Discovery, The Biodesign Institute, Arizona State University, Tempe, AZ, United States

Structural characterization of small molecules is a crucial component of organic synthesis. In this work, we applied microcrystal electron diffraction (MicroED) to analyze the structure of the product of an enzymatic reaction that was intended to produce the unnatural amino acid 2,4-dihydroxyphenylalanine (24DHF). Characterization of our isolated product with nuclear magnetic resonance spectroscopy (NMR) and mass spectrometry (MS) suggested that an isomer of 24DHF had been formed. Microcrystals present in the isolated product were then used to determine its structure to 0.62 Å resolution, which confirmed its identity as 2-amino-2-(2,4-dihydroxyphenyl)propanoic acid (24DHPA). Moreover, the MicroED structural model indicated that both enantiomeric forms of 24DHPA were present in the asymmetric unit. Notably, the entire structure determination process including setup, data collection, and refinement was completed in ~1 h. The MicroED data not only bolstered previous results obtained using NMR and MS but also immediately provided information about the stereoisomers present in the product, which is difficult to achieve using NMR and MS alone. Our results therefore demonstrate that MicroED methods can provide useful structural information on timescales that are similar to many commonly used analytical methods and can be added to the existing suite of small molecule structure determination tools in future studies.

Keywords: microcrystal electron diffraction (MicroED), electron diffraction, transmission electron microscope (TEM), organic synthesis, non-canonical amino acid (ncAA)

INTRODUCTION

The ability to unambiguously characterize the products of chemical reactions is of paramount importance in organic synthesis. A suite of analytical tools including mass spectrometry (MS) and spectroscopic techniques including ultraviolet and visible (UV-vis), infrared (IR) and nuclear magnetic resonance (NMR) are commonly used to characterize organic molecules. These methods are rapid, highly sensitive and—with the exception of MS—non-destructive to the sample. However, because the complete characterization of small molecules often requires the use of many, if not all, of the aforementioned techniques, researchers must possess the necessary expertise to interpret the diverse data generated using each of these analytical methods.

An alternative method that condenses a great deal of information into a single model is to directly determine a small molecule's structure using X-ray crystallography. Molecular structures not only provide the three-dimensional coordinates of each atom in the molecule, but also allow inferences about atom connectivity (i.e., bond number) and molecular packing interactions to be made. Despite these benefits, structural techniques suffer from limitations including the requirement of a large quantity of the small molecule and also that large, well-diffracting crystals are easily formed. These issues are especially problematic for natural products isolated directly from organisms or from very small-scale syntheses; only miniscule quantities of the target compound may be available in both cases. Furthermore, X-ray crystallographic methods are often more time consuming than other analytical methods and are therefore not commonly viewed as high-throughput for rapid small molecule analysis.

In recent years, technological advancements in the field of electron microscopy (EM) have expanded the utility of this technique into the field of protein structure determination (Nogales, 2016; Cheng et al., 2017). A major consequence of this is that access to electron microscopes has increased dramatically both at academic intuitions and through national cryo-EM user facilities. Furthermore, the recent development of techniques such as microcrystal electron diffraction (MicroED) have enabled the determination of the structures of both large biomolecules and small molecules in crystalline form (Gemmi et al., 2019; Nannenga and Gonen, 2019; Nannenga, 2020). Electron diffraction has been successfully applied to a wide variety of samples including proteins, peptides, small organic molecules, and inorganic materials (Mugnaioli et al., 2009, 2012, 2018; Zhang et al., 2013, 2018; Nannenga et al., 2014a,b; Rodriguez et al., 2015; Simancas et al., 2016; van Genderen et al., 2016; Clabbers et al., 2017, 2020; Krotee et al., 2017; Palatinus et al., 2017; Rozhdestvenskaya et al., 2017; Das et al., 2018; Gallagher-Jones et al., 2018; Gruene et al., 2018; Hughes et al., 2018; Jones et al., 2018; Liu and Gonen, 2018; Seidler et al., 2018; Brázda et al., 2019; Dick et al., 2019; Lanza et al., 2019; Warmack et al., 2019; Wennmacher et al., 2019; Xu et al., 2019; Zatsepin et al., 2019; Banihashemi et al., 2020; Levine et al., 2020; Zhu et al., 2020). A major benefit to this technique is that the micro and nanocrystals used for MicroED are several orders of magnitude smaller than those used in conventional X-ray crystallography. Furthermore, in the case of organic molecules, nanocrystals can be even be found in low quantities of synthesized or isolated material and be used directly for the collection of electron diffraction data (Gruene et al., 2018; Jones et al., 2018). Structural analysis using electron microscopes can therefore allow rapid, high-resolution structure determination of organic molecules. Moreover, this technique obviates the need to grow large crystals as is the case for X-ray studies. Thus, MicroED promises to be a powerful tool for organic chemistry and pharmaceutical research (Zhang et al., 2013; van Genderen et al., 2016; Das et al., 2018; Ting et al., 2019; Banihashemi et al., 2020; Levine et al., 2020).

Here we describe the direct characterization of a chemical intermediate obtained during an enzymatic semi-synthesis of a non-canonical amino acid using MicroED. Although evidence from traditional characterization methods (e.g., MS, NMR) provided insight into the structure of the intermediate, these results were incongruous with what would have been expected from an enzyme catalyzed chemical transformation. However, analysis of the intermediate using MicroED methods allowed the high-resolution structure to be determined in ∼1 h and confirmed the previous interpretation of the NMR data. Additionally, the MicroED structure indicated that the synthesized product was racemic, which was then confirmed by circular dichroism (CD). This work therefore serves to underscore the power of this burgeoning technique and further suggests that it can reasonably be added to the arsenal of analytical methods that are used to routinely characterize the structures of small molecules in a rapid manner.

MATERIALS AND METHODS

TPL Expression and Purification

A gene encoding tyrosine phenol-lyase (TPL) from *Citrobacter intermedius* was purchased from Integrated DNA Technologies, Inc. (Coralville, IA). The gene was cloned into a pET29b(+) expression vector (Novagen) using Gibson Assembly (New England Biolabs). After Sanger sequence verification, the plasmid was transformed into T7 Express Competent *Escherichia coli* cells (New England Biolabs). Because the pET29b(+) plasmid contains a kanamycin resistance gene, transformed cells were selected on agar plates containing kanamycin (50 μg/mL) to identify clones that contained the expression plasmid.

A single colony of T7 Express cells harboring the expression plasmid was used to inoculate 5 mL of 2xYT media containing kanamycin (50 μg/mL) and supplemented with 1 mM pyridoxal 5'-phosphate (PLP), a required cofactor of TPL. Cultures were incubated for 8 h at 37°C with 250 rpm shaking and ultimately reached an OD_{600} of ∼6.0. The 5 mL culture was then used to inoculate an additional 1 L of 2xYT containing kanamycin (50 μg/mL) and PLP (1 mM). This culture was then incubated at 30°C overnight; initial expression tests suggested that the addition of an inducer (e.g., isopropyl β-D-1-thiogalactopyranoside or lactose) was not necessary due to high basal levels of expression from the T7 promoter contained in the pET29b(+) plasmid. Cells were then harvested via centrifugation (5,000 × g, 15 min), resuspended in 50 mL cell lysis buffer (25 mM Tris HCl pH 8.0, 10 mM NaCl, 3 mM β-mercaptoethanol) and stored at −20°C overnight. The frozen cell suspension was thawed at room temperature and incubated at 37°C for 30 min with lysozyme (1 mg/mL). Both $MgCl_2$ (20 mM) and DNase (0.2 mg/mL; Sigma Aldrich) were then added to the cell lysate which was subsequently subjected to sonication (20 Hz, 10 min total time, 1 s on, 2 s off). The cell lysate was centrifuged (30,000 rpm for 20 min at 4°C) to remove cell debris.

TPL was then purified on a nickel-nitrilotriacetic acid resin (Ni-NTA, HisTrap FF, GE Healthcare). After loading on Ni-NTA, contaminant proteins were removed by washing the column with five column volumes (CV) of Ni-NTA buffer A (25 mM Tris-HCl pH 8.0, 20 mM Imidazole and 500 mM NaCl) followed by five CV of 90% Ni-NTA buffer A with 10% Ni-NTA buffer B (25 mM Tris-HCl pH 8.0, 500 mM Imidazole and 150 mM

NaCl). Proteins were then eluted with five column volumes of 100% Ni-NTA buffer B. Because PLP-bound TPL is bright yellow, fractions that were visibly yellow were collected and concentrated using ultrafiltration (30 kDa molecular weight cutoff, Sartorius Vivaspin). Proteins were then diluted 10-fold with anion exchange (IEC) loading buffer A (25 mM Tris-HCl pH 8.0, 10 mM NaCl) and further purified on IEC resin (HiTrap Q FF, GE Healthcare). The column was washed with five CV of IEC buffer A, followed by five CV of 90% IEC buffer A with 10% IEC buffer B (25 mM Tris-HCl pH 8.0, 500 mM NaCl). Proteins were then eluted with five column volumes of 100% IEC buffer B. Again, protein fractions that were found to be bright yellow were consolidated and concentrated to 500 μl using ultrafiltration as described above. The concentrated protein was then injected onto a size-exclusion column (Superdex 200 increase 10/300 gl, GE Healthcare) and eluted from the column with 25 mM Tris-HCl pH 8.0, 500 mM NaCl. Fractions that were bright yellow were collected, consolidated, and concentrated to a volume of ~1 mL. This protocol yielded ~20 mg of purified protein, which was then refrigerated at 4°C for use in subsequent experimental procedures. The purity of all samples was confirmed via SDS-PAGE (4% stacking/10% resolving, 100 V for 90 min) after each round of purification.

Small Molecule Synthesis and Purification

In this study, two variations of common protocols for the TPL-based synthesis of the tyrosine analogs were used:

Our first protocol followed the methods described by Kim and Cole (1998) and Kim et al. (2000). To a solution of TPL (190 nM; 30 units) in tris buffered saline (TBS, 25 mM Tris-HCl, pH 8.0, 500 mM NaCl, 5 mM β-mercaptoethanol) was added either resorcinol or phenol (10 mM), sodium pyruvate (60 mM), pyridoxal 5'-phosphate (40 μM), and ammonium chloride (30 mM). The reaction was stirred for 3 days at room temperature. The mixture was acidified to pH 3.0 with acetic acid and filtered over Celite. The filtrate was then extracted with ethyl acetate (3 × 500 mL) to remove excess resorcinol. The entire reaction mixture was then added to prewashed (6 N HCl, water, 6 N NaOH, water) Dowex 50W resin (20 g; Sigma Aldrich), washed with 5 CV of water and eluted with 10% aqueous ammonia. Elution fractions were subjected to a ninhydrin test, which provided a colorimetric indication of the presence of amino acid.

Synthesis of 2-Amino-2-(2,4-Dihydroxyphenyl)Propanoic Acid

The previously described protocol only indicated the presence of an amino acid in the control (see section Results and Discussion). We therefore employed a second method reported by Seisser et al. (Seisser et al., 2010). In this protocol, purified TPL (190 nM; 30 units) in TBS was added to a dialysis cassette (D-Tube™ Dialyzer Midi, MWCO 6–8 kDa, EMD Millipore) and was placed into 1 L of TBS containing resorcinol (50 mM, Sigma Aldrich) or phenol (50 mM, Oakwood Chemicals), sodium pyruvate (100 mM, Sigma-Aldrich), ammonium chloride (180 mM, Sigma-Aldrich),

and PLP (0.04 mM, Alfa Aesar). The reaction was covered with aluminum foil to block ambient light and stirred overnight. A white powder precipitated when either phenol (control) or resorcinol was subjected to the aforementioned conditions; both precipitants tested positive for an amino acid using ninhydrin. The precipitant from the resorcinol reaction was collected on filter paper, washed with water (3 × 50 ml) and dried under vacuum to yield 4.56 g of a white powder, which corresponds to a 46.28% yield. Analysis of the sample was then carried out using ^{1}H NMR and ESI-MS: ^{1}H NMR (D$_2$O, 500 MHz) δ 1.84 (s, 3H), 6.36 (d, 1H, J = 2.10 Hz), 6.41 (dd, 1H, J = 6.41 Hz and 10.80 Hz) and 7.23 (d, 1H, J = 8.60 Hz); ^{13}C NMR (D$_2$O, 500 MHz) δ 20.51, 59.27, 102.64, 107.41, 114.08, 128.68, 155.27, 158.39, and 174.93; ESI-MS calculated for C$_9$H$_{11}$NO$_4$ (M): 197.0688 Da; found: 197.0072 Da.
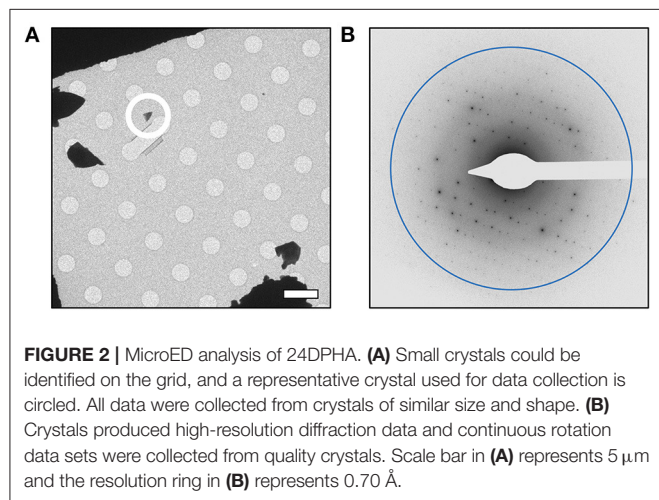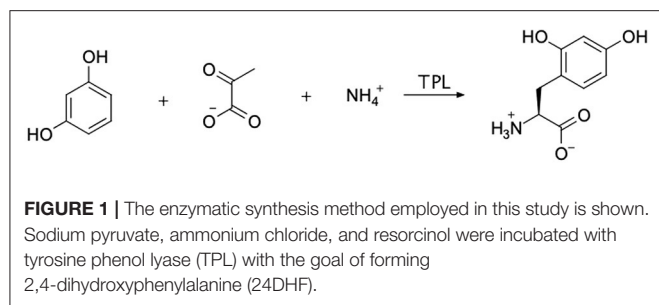
Thin Layer Chromatography of Products

Thin layer chromatography (TLC) was used as a high-throughput method for the detection of amino acid products. The precipitated reaction products were washed with water, dissolved in 1N NaOH, and run on silica plates (6:3:1 n-butanol:isopropanol:acetic acid). The silica gel plates were then heated to evaporate solvent and ammonia from the reaction mixture. Plates were then dipped in a solution of ninhydrin (1.5% w/v in a 3% v/v acetic acid:n-butanol) and were heated using a hot plate or heat gun; presence of a purple spot after heating was indicative of the presence of an amino acid product.

MicroED Sample Preparation, Data Collection, and Data Processing

Samples for MicroED analysis were prepared by placing a holey carbon EM grid directly into ~10 mg of the precipitated and dried white powder synthesized as described above. After gentle shaking of the grid in the powder, tweezers were used to extract the grid, and excess material was removed by gently tapping the tweezers. The grid was then loaded into a standard room temperature FEI TEM holder. MicroED data were collected at room temperature on an FEI Tecnai F20 equipped with a TVIPS XF-416 CMOS camera using standard low-dose MicroED data collection procedures (Nannenga et al., 2014a; Shi et al., 2016). Data were collected as the stage rotated at a continuous rate of 0.295 degrees per second and each frame was integrated over 2 s. To process the collected MicroED data sets, they were first converted to SMV format (Hattne et al., 2015). XDS (Kabsch, 2010) was used to index and integrate, and XSCALE was used to merge and scale the data from 3 crystals. The data were phased using SHELXT (Sheldrick, 2015), and the ShelXle (Hubschle et al., 2011) interface was used to refine the structure.

RESULTS AND DISCUSSION

Our primary goal was to synthesize the tyrosine analog, 2,4-dihydroxyphenylalanine (24DHF, **Figure 1**). A review of the literature suggested a number of possible strategies for achieving this using standard synthetic organic chemistry methods. However, we were drawn to an enzymatic semi-synthesis of this compound using tyrosine phenol lyase (TPL) from *Citrobacter*

FIGURE 1 | The enzymatic synthesis method employed in this study is shown. Sodium pyruvate, ammonium chloride, and resorcinol were incubated with tyrosine phenol lyase (TPL) with the goal of forming 2,4-dihydroxyphenylalanine (24DHF).

FIGURE 2 | MicroED analysis of 24DPHA. **(A)** Small crystals could be identified on the grid, and a representative crystal used for data collection is circled. All data were collected from crystals of similar size and shape. **(B)** Crystals produced high-resolution diffraction data and continuous rotation data sets were collected from quality crystals. Scale bar in **(A)** represents 5 μm and the resolution ring in **(B)** represents 0.70 Å.

TABLE 1 | Data collection and refinement statistics.

Data collection	
Excitation voltage	200 kV
Wavelength (Å)	0.0251
Number of crystals	3
Data processing	
Space group	$Pca2_1$
Unit cell length a, b, c (Å)	10.40, 22.80, 8.16
Angles $\alpha = \beta = \gamma$ (°)	90
Resolution (Å)	0.62
Number of reflections	24,851
Unique reflections	2,990
R_{obs} (%)	22.1 (96.0)
R_{meas} (%)	23.5 (114.9)
I/σ_I	5.32 (1.00)
$CC_{1/2}$ (%)	97.8 (51.3)
Completeness (%)	62.1 (42.3)
Structure refinement	
R1	0.1839 (0.1549 for $F_o > 4\sigma$)
wR2	0.4394
GooF	1.288

intermedius because the desired product could be synthesized in a single step from very inexpensive, commercially available starting materials. Namely, in previous reports, TPL was found to catalyze the synthesis of the 24DHF using only resorcinol, pyruvic acid and ammonia (Yamada et al., 1972; Sawada et al., 1975; Nagasawa et al., 1981) as reactants. These data were in contrast another report in which both resorcinol and 24DHF were suggested to represent potent inhibitors of TPL activity (Lambooy, 1954). Nonetheless, given the ease of synthesis, as well as the benefits of enzymatic rather than chemical synthesis (Koeller and Wong, 2001), we chose to explore an enzymatic route to this compound.

We tested two distinct protocols for 24DHF synthesis (see section Materials and Methods) that differed primarily in the concentration of reagents used. In a first protocol (Kim et al., 2000) with low reagent concentrations, no product was observed when resorcinol was used. However, when phenol (the native substrate of TPL) served as a positive control, the expected product, tyrosine, was generated. We then employed a second protocol reported by Seisser et al. (2010) in which high concentrations (50 mM or greater) of the reactants were used. In this case, both the phenol and resorcinol reactions yielded a white precipitate after only 2 h. Notably, both precipitates gave positive results when analyzed with ninhydrin on TLC, which suggested that an amino acid product had formed in both cases.
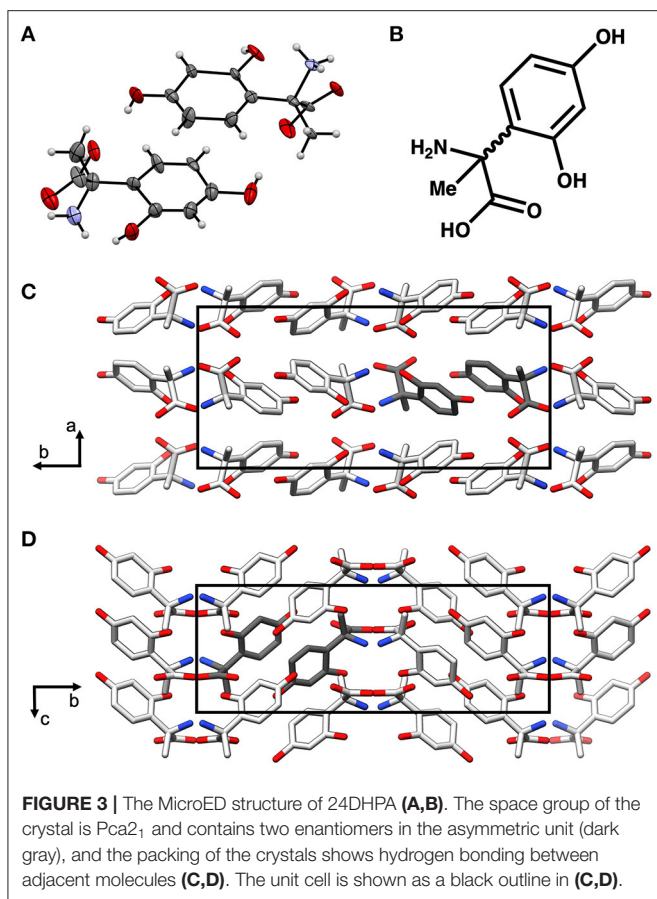
The product isolated from the reaction containing resorcinol was analyzed by ESI-mass spectrometry (ESI-MS), which indicated that our product had a mass of 197.01 Da. This is consistent with the calculated molecular mass of 24DHF (197.07 Da). Furthermore, analysis of this compound by ^{13}C NMR indicated the presence of 9 carbons, which is also consistent with the 24DHF structure (**Supplementary Figure 1**). However, the ^{1}H NMR spectrum (**Supplementary Figure 2**) was inconsistent with the predicted product. Namely, a singlet that integrated to three protons was observed at 1.84 ppm, which is indicative of a CH_3 functional group; no methyl groups were expected in the product. Furthermore, neither a CH_2 (corresponding to protons on the β-carbon) nor a CH proton peak (corresponding to the α-carbon proton) was observed in the ^{1}H spectrum. These data suggest that an isomer of 24DHF had been synthesized in lieu of the desired product.

In order to further characterize the isolated compound, we used MicroED for high-resolution structure determination. There are several methods for preparing small molecule samples for the TEM, including applying powdered sample directly to the grid, applying a crystalline suspension to the grid followed by drying, and direct crystal growth on the grid by solvent evaporation (van Genderen et al., 2016; Gruene et al., 2018; Jones et al., 2018; Banihashemi et al., 2020; Levine et al., 2020). For this analysis, preparing the EM grids with the sample was performed by simply placing the grids in a small amount of material as described above, a process which took less than 1 min. Upon loading the sample into the TEM, extremely small crystals could be found on the grid (**Figure 2A**), and the many of these diffracted to high-resolution (**Figure 2B**). Diffraction data were quickly collected from several crystals that all showed similar size and morphology. Ultimately, using standard procedures in XDS (Kabsch, 2010), data from 3 of the highest quality MicroED data sets were processed, all in space group 16

FIGURE 3 | The MicroED structure of 24DHPA **(A,B)**. The space group of the crystal is Pca2$_1$ and contains two enantiomers in the asymmetric unit (dark gray), and the packing of the crystals shows hydrogen bonding between adjacent molecules **(C,D)**. The unit cell is shown as a black outline in **(C,D)**.

FIGURE 4 | CD spectra of the racemic mixture of 2-amino-2-(2,4-dihydroxyphenyl)propanoic acid (24DHPA) and L-tyrosine (10 mM in 1 mM cuvette).

with similar unit cell parameters (**Supplementary Table 1**). These data were then merged into a final data set that was 62.1% complete (**Table 1**). Despite the low completeness, a solution could be found using SHELXT (Sheldrick, 2015), which allowed us to determine and refine the structure of the compound (**Figures 3A,B**). The structural model shows that instead of 24DHF, the resorcinol was added to the α-carbon to yield 2-amino-2-(2,4-dihydroxyphenyl)propanoic acid (24DHPA) (**Figure 3B**), which confirmed the unexpected findings from NMR.

An additional finding from the high-resolution structure was that both enantiomers were observed in the asymmetric unit, suggesting that the compound was present as a racemic mixture. This was subsequently confirmed using circular dichroism (Shinitzky et al., 2004) (CD, 10 mM sample in 300 μL 1 M HCl), which resulted in a featureless spectrum (**Figure 4**). Because racemic mixtures of compounds are difficult to identify with NMR without first subjecting the sample to a chiral derivatization agent, the use of electron diffraction has the advantage of providing this information concurrently with the determination of the structure.

Furthermore, the fact that a racemic mixture of products was observed seems inconsistent with a TPL-based enzymatic synthesis. Namely, because TPL's native substrate is the L-amino acid tyrosine, a single product with L- stereochemistry
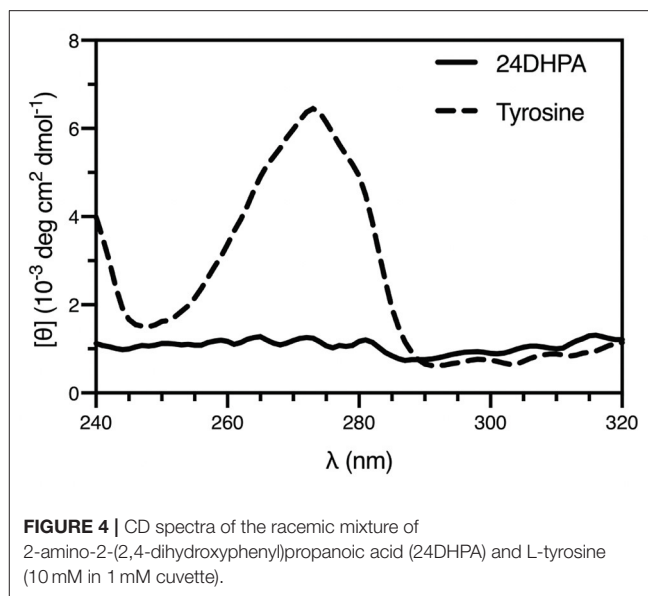
should have been produced using these conditions. As mentioned above, both resorcinol and the desired 24DHF product have been previously suggested to be inhibitors of TPL (Lambooy, 1954). That we observed a racemic product supports the possibility that either the resorcinol or a small amount of 24DHF synthesized by TPL in an initial reaction may have inhibited TPL and precluded enzymatic synthesis by blocking access to the active site. Although beyond the scope of this study, the mechanism of the reaction that led to the aberrant product could warrant additional inquiry.

CONCLUSION

In this work, we demonstrate the utility of MicroED as a rapid method for determining the structure of a synthetic product. Although standard analytical techniques (e.g., ^{1}H NMR) indicated that our isolated product was not 24DHF as we had set out to make, the MicroED data rapidly confirmed our interpretation. Furthermore, the structure of the aberrant product that was determined using MicroED methods immediately suggested the presence of a racemic mixture of products, which obviated the need to carry out an analysis of the stereochemical properties of the product using chiral separation or polarimetry. The MicroED process, including sample preparation, data collection, data processing and structure refinement, was completed in ~1 h and yielded a structure at 0.62Å resolution. Thus, our results further confirm that MicroED represents a rapid method of gaining insight into the structural features of organic molecules that may prove difficult to obtain using more traditional methods. While it is unlikely that structure determination by electron diffraction will supplant more commonly used analytical techniques, we believe it could be

reasonably added to the existing set of analytical tools in future studies.

DATA AVAILABILITY STATEMENT

The raw data supporting the conclusions of this article will be made available by the authors, without undue reservation.

AUTHOR CONTRIBUTIONS

All authors contributed to the planning and conducting of the experiments, the analysis of results, and writing the manuscript.

SUPPLEMENTARY MATERIAL

The Supplementary Material for this article can be found online at: https://www.frontiersin.org/articles/10.3389/fmolb.2020.609999/full#supplementary-material

Supplementary Figure 1 | ^{13}C NMR spectrum of 2-amino-2-(2,4-dihydroxyphenyl)propanoic acid (24DHPA) in D_2O.

Supplementary Figure 2 | ^{1}H NMR spectrum of 2-amino-2-(2,4-dihydroxyphenyl)propanoic acid (24DHPA) in D_2O.

Supplementary Table 1 | Data processing statistics for individual crystals using XDS and XSCALE.

REFERENCES

Banihashemi, F., Bu, G., Thaker, A., Williams, D., Lin, J. Y. S., and Nannenga, B. L. (2020). Beam-sensitive metal-organic framework structure determination by microcrystal electron diffraction. *Ultramicroscopy* 216:113048. doi: 10.1016/j.ultramic.2020.113048

Brázda, P., Palatinus, L., and Babor, M. (2019). Electron diffraction determines molecular absolute configuration in a pharmaceutical nanocrystal. *Science* 364, 667–669. doi: 10.1126/science.aaw2560

Cheng, Y., Glaeser, R. M., and Nogales, E. (2017). How cryo-EM became so hot. *Cell* 171, 1229–1231. doi: 10.1016/j.cell.2017.11.016

Clabbers, M. T. B., Fisher, S. Z., Coinçon, M., Zou, X., and Xu, H. (2020). Visualizing drug binding interactions using microcrystal electron diffraction. *Commun. Biol.* 3:417. doi: 10.1038/s42003-020-01155-1

Clabbers, M. T. B., van Genderen, E., Wan, W., Wiegers, E. L., Gruene, T., and Abrahams, J. P. (2017). Protein structure determination by electron diffraction using a single three-dimensional nanocrystal. *Acta Crystallogr. D Struct. Biol.* 73(Pt. 9), 738–748. doi: 10.1107/S2059798317010348

Das, P. P., Mugnaioli, E., Nicolopoulos, S., Tossi, C., Gemmi, M., Galanis, A., et al. (2018). Crystal structures of two important pharmaceuticals solved by 3D precession electron diffraction tomography. *Org. Process Res. Dev.* 22, 1365–1372. doi: 10.1021/acs.oprd.8b00149

Dick, M., Sarai, N. S., Martynowycz, M. W., Gonen, T., and Arnold, F. H. (2019). Tailoring tryptophan synthase TrpB for selective quaternary carbon bond formation. *J. Am. Chem. Soc.* 141, 19817–19822. doi: 10.1021/jacs.9b09864

Gallagher-Jones, M., Glynn, C., Boyer, D. R., Martynowycz, M. W., Hernandez, E., Miao, J., et al. (2018). Sub-angstrom cryo-EM structure of a prion protofibril reveals a polar clasp. *Nat. Struct. Mol. Biol.* 25, 131–134. doi: 10.1038/s41594-017-0018-0

Gemmi, M., Mugnaioli, E., Gorelik, T. E., Kolb, U., Palatinus, L., Boullay, P., et al. (2019). 3D electron diffraction: the nanocrystallography revolution. *ACS Centrl. Sci.* 5, 1351–1329. doi: 10.1021/acscentsci.9b00394

Gruene, T., Wennmacher, J. T. C., Zaubitzer, C., Holstein, J. J., Heidler, J., Fecteau-Lefebvre, A., et al. (2018). Rapid structure determination of microcrystalline molecular compounds using electron diffraction. *Angew. Chem. Int. Ed. Engl.* 57, 16313–16317. doi: 10.1002/anie.201811318

Hattne, J., Reyes, F. E., Nannenga, B. L., Shi, D., de la Cruz, M. J., Leslie, A. G., et al. (2015). MicroED data collection and processing. *Acta Crystallogr. A Found Adv.* 71(Pt. 4), 353–360. doi: 10.1107/S2053273315010669

Hubschle, C. B., Sheldrick, G. M., and Dittrich, B. (2011). ShelXle: a Qt graphical user interface for SHELXL. *J. Appl. Crystallogr.* 44(Pt. 6), 1281–1284. doi: 10.1107/S0021889811043202

Hughes, M. P., Sawaya, M. R., Boyer, D. R., Goldschmidt, L., Rodriguez, J. A., Cascio, D., et al. (2018). Atomic structures of low-complexity protein segments reveal kinked beta sheets that assemble networks. *Science* 359, 698–701. doi: 10.1126/science.aan6398

Jones, C. G., Martynowycz, M. W., Hattne, J., Fulton, T. J., Stoltz, B. M., Rodriguez, J. A., et al. (2018). The cryoEM method microED as a powerful tool for small molecule structure determination. *ACS Centrl. Sci.* 4, 1587–1592. doi: 10.1021/acscentsci.8b00760

Kabsch, W. (2010). Xds. *Acta Crystallogr. D Biol. Crystallogr.* 66(Pt. 2), 125–132. doi: 10.1107/S0907444909047337

Kim, K., and Cole, P. A. (1998). Kinetic analysis of a protein tyrosine kinase reaction transition state in the forward and reverse directions. *J. Am. Chem. Soc.* 120, 6851–6858. doi: 10.1021/ja9808393

Kim, K., Parang, K., Lau, O. D., and Cole, P. A. (2000). Tyrosine analogues as alternative substrates for protein tyrosine kinase Csk: insights into substrate selectivity and catalytic mechanism. *Bioorg. Med. Chem.* 8, 1263–1268. doi: 10.1016/S0968-0896(00)00053-5

Koeller, K. M., and Wong, C. H. (2001). Enzymes for chemical synthesis. *Nature* 409, 232–240. doi: 10.1038/35051706

Krotee, P., Rodriguez, J. A., Sawaya, M. R., Cascio, D., Reyes, F. E., Shi, D., et al. (2017). Atomic structures of fibrillar segments of hIAPP suggest tightly mated beta-sheets are important for cytotoxicity. *Elife* 6:e19273. doi: 10.7554/eLife.19273

Lambooy, J. P. (1954). The syntheses, paper chromatography and substrate specificity for tyrosinase of 2,3-, 2,4-, 2,5-, 2,6- and 3,5-dihydroxyphenylalanines. *J. Am. Chem. Soc.* 76, 133–138. doi: 10.1021/ja01630a037

Lanza, A., Margheritis, E., Mugnaioli, E., Cappello, V., Garau, G., and Gemmi, M. (2019). Nanobeam precession-assisted 3D electron diffraction reveals a new polymorph of hen egg-white lysozyme. *IUCrJ* 6, 178–188. doi: 10.1107/S2052252518017657

Levine, A. M., Bu, G., Biswas, S., Tsai, E. H. R., Braunschweig, A. B., and Nannenga, B. L. (2020). Crystal structure and orientation of organic semiconductor thin films by microcrystal electron diffraction and grazing-incidence wide-angle X-ray scattering. *Chem. Commun.* 56, 4204–4207. doi: 10.1039/D0CC00119H

Liu, S., and Gonen, T. (2018). MicroED structure of the NaK ion channel reveals a Na$^+$ partition process into the selectivity filter. *Commun. Biol.* 1:38. doi: 10.1038/s42003-018-0040-8

Mugnaioli, E., Andrusenko, I., Schuler, T., Loges, N., Dinnebier, R. E., Panthofer, M., et al. (2012). Ab initio structure determination of vaterite by automated electron diffraction. *Angew. Chem. Int. Edn.* 51, 7041–7045. doi: 10.1002/anie.201200845

Mugnaioli, E., Gemmi, M., Tu, R., David, J., Bertoni, G., Gaspari, R., et al. (2018). Ab initio structure determination of Cu2–xTe plasmonic nanocrystals by precession-assisted electron diffraction tomography and HAADF-STEM imaging. *Inorg. Chem.* 57, 10241–10248. doi: 10.1021/acs.inorgchem.8b01445

Mugnaioli, E., Gorelik, T., and Kolb, U. (2009). "Ab initio" structure solution from electron diffraction data obtained by a combination of automated diffraction tomography and precession technique. *Ultramicroscopy* 109, 758–765. doi: 10.1016/j.ultramic.2009.01.011

Nagasawa, T., Utagawa, T., Goto, J., Kim, C. J., Tani, Y., Kumagai, H., et al. (1981). Syntheses of L-tyrosine-related amino acids by tyrosine phenol-lyase of citrobacter intermedius. *Eur. J. Biochem.* 117, 33–40. doi: 10.1111/j.1432-1033.1981.tb06299.x

Nannenga, B. L. (2020). MicroED methodology and development. *Struct Dyn* 7:014304. doi: 10.1063/1.5128226

Nannenga, B. L., and Gonen, T. (2019). The cryo-EM method microcrystal electron diffraction (microED). *Nat. Methods* 16, 369–379. doi: 10.1038/s41592-019-0395-x

Nannenga, B. L., Shi, D., Hattne, J., Reyes, F. E., and Gonen, T. (2014a). Structure of catalase determined by microED. *Elife* 3:e03600. doi: 10.7554/eLife.03600

Nannenga, B. L., Shi, D., Leslie, A. G., and Gonen, T. (2014b). High-resolution structure determination by continuous-rotation data collection in microED. *Nat. Methods* 11, 927–930. doi: 10.1038/nmeth.3043

Nogales, E. (2016). The development of cryo-EM into a mainstream structural biology technique. *Nat. Methods* 13, 24–27. doi: 10.1038/nmeth.3694

Palatinus, L., Brazda, P., Boullay, P., Perez, O., Klementova, M., Petit, S., et al. (2017). Hydrogen positions in single nanocrystals revealed by electron diffraction. *Science* 355, 166–169. doi: 10.1126/science.aak9652

Rodriguez, J. A., Ivanova, M. I., Sawaya, M. R., Cascio, D., Reyes, F. E., Shi, D., et al. (2015). Structure of the toxic core of alpha-synuclein from invisible crystals. *Nature* 525, 486–490. doi: 10.1038/nature15368

Rozhdestvenskaya, I. V., Mugnaioli, E., Schowalter, M., Schmidt, M. U., Czank, M., Depmeier, W., et al. (2017). The structure of denisovite, a fibrous nanocrystalline polytypic disordered 'very complex' silicate, studied by a synergistic multi-disciplinary approach employing methods of electron crystallography and X-ray powder diffraction. *IUCrJ* 4, 223–242. doi: 10.1107/S2052252517002585

Sawada, S., Kumagai, H., Yamada, H., and Hill, R. K. (1975). Stereochemistry of beta-replacement reactions catalyzed by tyrosine phenol-lyase. *J. Am. Chem. Soc.* 97, 4334–4337. doi: 10.1021/ja00848a033

Seidler, P. M., Boyer, D. R., Rodriguez, J. A., Sawaya, M. R., Cascio, D., Murray, K., et al. (2018). Structure-based inhibitors of tau aggregation. *Nat. Chem.* 10, 170–176. doi: 10.1038/nchem.2889

Seisser, B., Zinkl, R., Gruber, K., Kaufmann, F., Hafner, A., and Kroutil, W. (2010). Cutting long syntheses short: access to non-natural tyrosine derivatives employing an engineered tyrosine phenol lyase. *Adv. Synth. Catal.* 352, 731–736. doi: 10.1002/adsc.200900826

Sheldrick, G. M. (2015). SHELXT - integrated space-group and crystal-structure determination. *Acta Crystallogr. A Found Adv.* 71(Pt. 1), 3–8. doi: 10.1107/S2053273314026370

Shi, D., Nannenga, B. L., de la Cruz, M. J., Liu, J., Sawtelle, S., Calero, G., et al. (2016). The collection of MicroED data for macromolecular crystallography. *Nat. Protoc.* 11, 895–904. doi: 10.1038/nprot.2016.046

Shinitzky, M., Elitzur, A. C., and Deamer, D. W. (2004). "Chapter 27 - deviation from physical identity between D- and L-tyrosine," in *Progress in Biological Chirality,* eds G. Pályi, C. Zucchi, and L. Caglioti (Oxford: Elsevier Science Ltd), 329–337.

Simancas, J., Simancas, R., Bereciartua, P. J., Jorda, J. L., Rey, F., Corma, A., et al. (2016). Ultrafast electron diffraction tomography for structure determination of the new zeolite ITQ-58. *J. Am. Chem. Soc.* 138, 10116–10119. doi: 10.1021/jacs.6b06394

Ting, C. P., Funk, M. A., Halaby, S. L., Zhang, Z., Gonen, T., and van der Donk, W. A. (2019). Use of a scaffold peptide in the biosynthesis of amino acid–derived natural products. *Science* 365, 280–284. doi: 10.1126/science.aau6232

van Genderen, E., Clabbers, M. T., Das, P. P., Stewart, A., Nederlof, I., Barentsen, K. C., et al. (2016). Ab initio structure determination of nanocrystals of organic pharmaceutical compounds by electron diffraction at room temperature using a Timepix quantum area direct electron detector. *Acta Crystallogr. A Found Adv.* 72(Pt. 2), 236–242. doi: 10.1107/S2053273315022500

Warmack, R. A., Boyer, D. R., Zee, C.-T., Richards, L. S., Sawaya, M. R., Cascio, D., et al. (2019). Structure of amyloid-β (20-34) with Alzheimer's-associated isomerization at Asp23 reveals a distinct protofilament interface. *Nat. Commun.* 10:3357. doi: 10.1038/s41467-019-11183-z

Wennmacher, J. T. C., Zaubitzer, C., Li, T., Bahk, Y. K., Wang, J., van Bokhoven, J. A., et al. (2019). 3D-structured supports create complete data sets for electron crystallography. *Nat. Commun.* 10:3316. doi: 10.1038/s41467-019-11326-2

Xu, H., Lebrette, H., Clabbers, M. T. B., Zhao, J., Griese, J. J., Zou, X., et al. (2019). Solving a new R2lox protein structure by microcrystal electron diffraction. *Sci. Adv.* 5:eaax4621. doi: 10.1126/sciadv.aax4621

Yamada, H., Kumagai, H., Kashima, N., Torii, H., Enei, H., and Okumura, S. (1972). Synthesis of L-tyrosine from pyruvate, ammonia and phenol by crystalline tyrosine phenol lyase. *Biochem. Biophys. Res. Commun.* 46, 370–374. doi: 10.1016/S0006-291X(72)80148-7

Zatsepin, N. A., Li, C., Colasurd, P., and Nannenga, B. L. (2019). The complementarity of serial femtosecond crystallography and MicroED for structure determination from microcrystals. *Curr. Opin. Struct. Biol.* 58, 286–293. doi: 10.1016/j.sbi.2019.06.004

Zhang, C., Kapaca, E., Li, J., Liu, Y., Yi, X., Zheng, A., et al. (2018). An extra-large-pore zeolite with 24×8×8-ring channels using a structure-directing agent derived from traditional chinese medicine. *Angew. Chem. Int. Edn.* 57, 6486–6490. doi: 10.1002/anie.201801386

Zhang, Y. B., Su, J., Furukawa, H., Yun, Y. F., Gandara, F., Duong, A., et al. (2013). Single-crystal structure of a covalent organic framework. *J. Am. Chem. Soc.*135, 16336–16339. doi: 10.1021/ja409033p

Zhu, L., Bu, G., Jing, L., Shi, D., Lee, M.-Y., Gonen, T., et al. (2020). Structure determination from lipidic cubic phase embedded microcrystals by microED. *Structure* 28, 1149–1159.e44. doi: 10.1016/j.str.2020.07.006